ADVANCES IN ATMOSPHERIC SCIENCES, VOL. 34, APRIL 2017, 482–496

• **Original Paper** •

Numerical Simulation of the Rapid Intensification of Hurricane Katrina (2005): Sensitivity to Boundary Layer Parameterization Schemes

Jianjun LIU[1,2,4], Feimin ZHANG[3,2], and Zhaoxia PU[*2]

[1]*Nanjing University of Information and Technology, Nanjing, Jiangsu* 210044*, China*
[2]*Department of Atmospheric Sciences, University of Utah, Salt Lake City, Utah* 84112*, USA*
[3]*College of Atmospheric Sciences, Lanzhou University, Lanzhou, Gansu* 73000*, China*
[4]*Ningxia Meteorological Bureau, Yinchuan, Ningxia* 750002*, China*

(Received 9 August 2016; revised 20 October 2016; accepted 10 November 2016)

ABSTRACT

Accurate forecasting of the intensity changes of hurricanes is an important yet challenging problem in numerical weather prediction. The rapid intensification of Hurricane Katrina (2005) before its landfall in the southern US is studied with the Advanced Research version of the WRF (Weather Research and Forecasting) model. The sensitivity of numerical simulations to two popular planetary boundary layer (PBL) schemes, the Mellor–Yamada–Janjic (MYJ) and the Yonsei University (YSU) schemes, is investigated. It is found that, compared with the YSU simulation, the simulation with the MYJ scheme produces better track and intensity evolution, better vortex structure, and more accurate landfall time and location. Large discrepancies (e.g., over 10 hPa in simulated minimum sea level pressure) are found between the two simulations during the rapid intensification period. Further diagnosis indicates that stronger surface fluxes and vertical mixing in the PBL from the simulation with the MYJ scheme lead to enhanced air–sea interaction, which helps generate more realistic simulations of the rapid intensification process. Overall, the results from this study suggest that improved representation of surface fluxes and vertical mixing in the PBL is essential for accurate prediction of hurricane intensity changes.

Key words: hurricane, PBL, numerical simulation, hurricane intensity change

Citation: Liu, J. J., F. M. Zhang, and Z. X. Pu, 2017: Numerical simulations of the rapid intensification of Hurricane Katrina (2005): Sensitivity to boundary layer parameterization schemes. *Adv. Atmos. Sci.*, **34**(4), 482–496, doi: 10.1007/s00376-016-6209-5.

1. Introduction

A hurricane can cause severe loss of life and property damage, especially when it approaches coastal regions or makes landfall. Accurate prediction of the track and intensity of a hurricane before and near its landfall is essential (Landsea, 1993; Pielke and Pielke, 1997; Elsberry, 2005).

Over the past two decades, hurricane track forecasts have improved substantially through better understanding of overall storm dynamics, improved numerical models, and observation technologies. However, the accurate prediction of intensity change, especially rapid intensification (RI), still presents a challenge in research and operational communities (e.g., Marks and Shay, 1998; Rogers et al., 2006, 2013; Gall et al., 2013). This is mainly because of insufficient understanding regarding the physical processes associated with hurricane intensity changes (Davis and Bosart, 2002), but also because of uncertainties related to physical parameterizations in numerical models (Karyampudi et al., 1998; Houze et al., 2006).

Hurricane RI is usually defined as an increase of 30 kt (1 kt = 0.5144 m s^{-1}) in the maximum sustained surface wind or a decrease of 24 hPa in the minimum central pressure over 24 h (Kaplan and DeMaria, 2003; Kaplan et al., 2010). So far, physical processes associated with RI are not well understood (Kieper and Jiang, 2012). Previous studies have shown that warm sea surface temperature (SST), high low- to mid-level moisture, enhanced heat and moisture flux, and low vertical wind shear, are the large-scale environmental condition necessary for RI (Gray, 1968; Bosart et al., 2000; Jiang et al., 2011). Mesoscale phenomena, such as convective bursts near the eyewall, vertical hot towers, a precipitation ring pattern, and lightning activity, are also closely related to the hurricane RI process. For instance, the intensification of a tropical cyclone (TC) is closely related to the existence of hot towers in the eyewall (Kelley et al., 2004, 2005), and the probability of RI increases when hot towers exist in the inner core (Jiang, 2012). Hendricks et al. (2004) and Montgomery et al. (2006a) proposed that intense "vertical hot towers" might be

* Corresponding author: Zhaoxia PU
Email: zhaoxia.pu@utah.edu

a missing link in initiating TC genesis and RI. Results from Cecil and Zipser (1999) and Guimond et al. (2010) further emphasized the importance of net heating from both stratiform and convective heating to TC intensification. Recent studies (e.g., Fierro et al., 2011; DeMaria et al., 2012) have also found that electrical activity is closely related to hurricane intensity and is helpful for the short-term prediction of RI.

Among the difficulties in accurate prediction of hurricane intensity changes, hurricane RI prior to landfall is even more challenging for warning decisions, but also critical, as the damage from a landfalling hurricane is highly related to its intensity (Landsea, 1993). Many landfalling hurricanes experience an intensification prior to their landfall (e.g., Lin et al., 2009), and the problem has not yet received much attention in previous studies, many of which have emphasized RI right after the genesis of a TC over the open ocean.

To improve forecasts of hurricane intensity changes, physical processes associated with hurricane intensifications have been investigated in numerous previous studies (e.g., Malkus, 1958; Frank, 1977; Willoughby, 1988; Frank and Ritchie, 1999; Montgomery et al., 2006b; Elsberry et al., 2013). It has been recognized that physical parameterization schemes have a significant impact on the accuracy of forecasts of hurricane intensity and structure changes. Among all these physical processes, planetary boundary layer (PBL) processes play an important role in hurricane evolution. Recent field programs, such as CBLAST (Coupled Boundary Layer Air–Sea Transfer; Black et al., 2007), have proven that PBL processes play a significant role in air–sea interactions during hurricane evolution. Numerical studies have also pointed out that numerical simulations and forecasts of hurricanes are very sensitive to the specification of PBL parameterization schemes. For instance, Braun and Tao (2000) conducted experiments to determine the sensitivity of hurricane simulations to different PBL schemes in the Fifth-generation Pennsylvania State University-National Center for Atmospheric Research Mesoscale Model (MM5), showing that hurricane intensity is closely related to the strength of the vertical mixing in each PBL scheme. Li and Pu (2008) simulated the early RI of Hurricane Emily (2005) with different PBL schemes in the Advanced Research version of the Weather Research and Forecasting (WRF; Skamarock et al., 2008) model (WRF-ARW). They found that the early RI of Hurricane Emily (2005) was very sensitive to the choice of PBL scheme and that there were differences up to 19 hPa in the simulated mean sea level pressure between the Yonsei University (YSU) and Mellor–Yamada–Janjic (MYJ) schemes during the 30-h forecast period. Nolan et al. (2009) evaluated the YSU and MYJ schemes in the WRF model using *in situ* data obtained from aircraft. Results showed that both schemes reproduced certain unique features of the hurricane boundary layer. However, the MYJ scheme consistently produced larger frictional tendencies in the boundary layer than the YSU scheme, leading to a stronger low-level inflow and a stronger azimuthal wind speed. Smith and Thomsen (2010) compared hurricane simulations with different PBL schemes in an idealized model and found significant variation in storm structure, intensity, and rate of intensification. Zhu et al. (2014) showed that the vertical turbulent mixing scheme not only substantially affects the subgrid-scale vertical transport of heat and moisture but also has an important bearing on the storm's axisymmetric structure, eyewall mesovortices, and other resolved asymmetric features in the vicinity of the hurricane eyewall. The budget analysis by Rotunno and Bryan (2012) suggested that, apart from vertical diffusion in the PBL, horizontal diffusion also plays an important role in hurricane intensity changes. Kepert (2012) reviewed and evaluated PBL parameterizations with a diagnostic TC model. Results indicated that the Louis scheme and a higher-order closure scheme, such as the MYJ scheme, are suitable and recommended for hurricane simulation.

In light of the above, in this study we examine the role of PBL processes in predicting the RI of Hurricane Katrina (2005) prior to its landfall. Specifically, we perform numerical simulation experiments to evaluate the sensitivity of numerical simulations of Hurricane Katrina (2005) to PBL schemes in the WRF model. Two popular PBL schemes, the YSU (Troen and Mahrt, 1986; Noh et al., 2003; Hong et al., 2006) and MYJ (Mellor and Yamada, 1982; Janjić, 2002) schemes, are examined. These two schemes have been widely used in TC simulations with the WRF model in recent years (Kepert, 2012). The evolution of the hurricane's intensity and structure during its RI prior to landfall, the sensitivity of the simulation to different PBL schemes, and the effect of boundary layer processes on RI, are investigated.

The paper is organized as follows. Section 2 gives a brief overview of Hurricane Katrina (2005). Section 3 introduces the configuration of the numerical simulations and the differences between the two popular PBL schemes. Section 4 illustrates the overall simulation results. Section 5 demonstrates the influence of the PBL schemes on the numerical simulations. Concluding remarks are provided in section 6.

2. Brief overview of Hurricane Katrina (2005)

Hurricane Katrina (2005) caused catastrophic damage and a large loss of life. It was one of the five deadliest hurricanes ever to strike the United States. The National Hurricane Center (NHC) designated it as a tropical depression (TD) at 1800 UTC 23 August 2005 over the southeastern Bahamas, and then a tropical storm (TS) at 1200 UTC 24 August. During its life cycle, Katrina (2005) made two landfalls. The first was in southern Florida shortly before 0000 UTC 26 August, when it was a category-1 hurricane. After the first landfall, Katrina (2005) moved over the warm ocean of the Gulf of Mexico, where it underwent two periods of RI and became a category-5 hurricane between 26 August and 28 August. It then made its second landfall at 1100 UTC 29 August in New Orleans, Louisiana, USA.

In this study, we choose to focus on the period before Katrina (2005)'s second landfall to demonstrate the effects of atmospheric boundary layer processes on Katrina (2005)'s

RI and structure changes. The simulation period covers 1800 UTC 27 August to 0000 UTC 30 August 2005, including the RI period prior to its landfall from 1800 UTC 27 August to 1800 UTC 28 August, with a rapid decrease of 46 hPa in minimum sea level pressure and a rapid increase of 50 kt in maximum surface wind speed. Figure 1a shows the track of Katrina (2005) from the NHC best track during the simulation period and the SST at 0000 UTC 27 August 2015.

3. Description of numerical simulations and PBL schemes

3.1. *WRF model and simulation configuration*

WRF-ARW (Skamarock et al., 2008) is employed for numerical simulation. WRF-ARW is a nonhydrostatic model and uses a mass (hydrostatic pressure) vertical coordinate. WRF-ARW also carries multiple physical options for cumulus, microphysics, PBL, and radiation physical processes. Details of the model are provided in Skamarock et al. (2008).

A total of 60 vertical σ-levels are set, with the top of the model at 50 hPa. A two-way interaction, three-level nested domain technique is used with horizontal grid spacing of 27, 9, and 3 km for Domain 1, Domain 2 and Domain 3, respectively (Fig. 1b). Physical parameterization options include WSM6 (WRF single-moment 6-class microphysics scheme; Hong and Lim, 2006), the Kain–Fritsch cumulus parameterization scheme (Kain and Fritsch, 1993), the Noah land surface model (Chen and Dudhia, 2001), the RRTM (Rapid Radiative Transfer Model; Mlawer et al., 1997) for longwave radiation, and the Dudhia shortwave radiation scheme (Dudhia, 1989). The cumulus scheme is used in the 27- and 9-km grid spacing domains only (Domain 1 and Domain 2). As mentioned, two popular, widely used PBL schemes, the MYJ and YSU schemes, are applied for two sets of simulations, respectively.

The initial and boundary conditions are derived from the NCEP's GFS (Global Forecast System) FNL (final analysis) at a resolution of $1^\circ \times 1^\circ$. The WRF model is initiated at 0000 UTC 27 August to spin up the vortices. Then, the available conventional observations are assimilated using the WRF three-dimensional variational data assimilation system at 1200 UTC and 1800 UTC 27 August in the WRF model domains, followed by WRF simulations until 0000 UTC 30 August, shortly after Katrina (2005)'s landfall.

3.2. *The MYJ and YSU boundary layer schemes*

In PBL parameterization, the relationship between prognostic mean variables (c) such as zonal wind (u), meridian wind (v), potential temperature (θ) and water vapor (q) ($c : u, v, \theta, q$) and subgrid-scale turbulent fluxes (second momentum terms, $\overline{w'c'}$) can be simply expressed as

$$\frac{\partial c}{\partial t} = -\frac{\partial}{\partial z}\overline{w'c'}\,, \tag{1}$$

where w' is the perturbation of vertical velocity.

The subgrid-scale turbulent fluxes ($\overline{w'c'}$) can be further defined as

$$-\overline{w'c'} = K_c \frac{\partial c}{\partial z}\,, \tag{2}$$

where K_c is the eddy diffusivity for variable c, and we denote K_m as the momentum eddy diffusivity for u and v, and K_h as the thermal eddy diffusivity for θ and q.

The MYJ scheme is classified as a 1.5-order turbulent local closure scheme, since the subgrid-scale turbulent fluxes are parameterized with other prognostic equations such as the turbulent kinetic energy (TKE) equation (Mellor and Yamada, 1982). The YSU scheme is a typical first-order nonlocal closure scheme, since the subgrid-scale turbulent fluxes are explicitly parameterized with K-theory approximation and do not require any additional prognostic equations (Troen and Mahrt, 1986). Therefore, the eddy diffusivity defined in Eq. (2) is fundamentally different in the two schemes.

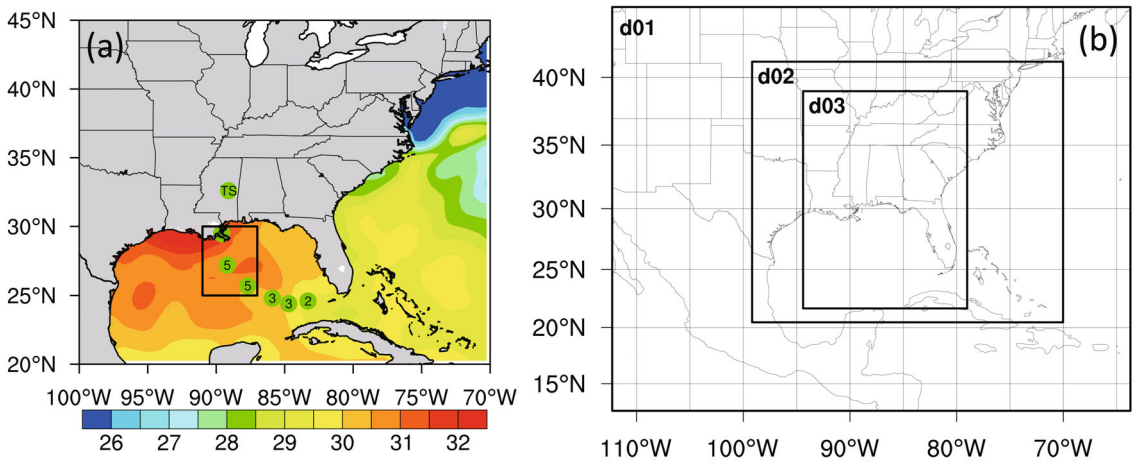

Fig. 1. (a) Best-track position of Hurricane Katrina during 27–31 August 2005. Color-shaded contours denote SST (units: °C) at 0000 UTC 27 August 2005. The small black box indicates the rapid intensification period. The numbers and "TS" denotes the intensity of Katrina (2005). (b) Locations of the model domains for the WRF simulations, d01, d02, and d03 represent the outer domain, the middle domain and the inner domain, respectively.

The eddy diffusivity for momentum (K_m) in the YSU scheme is defined as

$$K_m = kw_s z\left(1-\frac{z}{h}\right)p\ , \tag{3}$$

where w_s represents the mixed layer velocity scale (Hong et al., 2006); p is the profile shape exponent, taken to be 2; k is the Von Kármán constant (= 0.4); z is the height from the surface; and h is the height of the PBL. The thermal eddy diffusivity (K_h) is proportional to K_m according to the Prandtl number.

The eddy diffusivity in the MYJ scheme is defined as

$$K_c = l\sqrt{e}S_c\ , \tag{4}$$

where l is the mixing length, and S_c is the proportional coefficient for momentum and thermal diffusivity, which is determined by TKE [denoted by e in Eq. (4)].

Clearly, eddy diffusivity is determined by the TKE budget in the MYJ scheme, but not in the YSU scheme. In addition, in the YSU scheme, the turbulent flux of each grid involves the influence of the flux from its neighboring grids at multiple vertical levels. This is different from the treatment in MYJ, in which the turbulent flux depends on the local TKE and only those vertical levels that are directly adjacent to a given point affect variables at that point (Cohen et al., 2015). Overall, the different approach for parameterizing turbulence exchange in the PBL leads to a fundamental difference in the vertical mixing effects in the two PBL schemes.

Moreover, the PBL height (PBLH) in the MYJ scheme is defined as the lowest model level above the surface at which TKE approaches its prescribed lower bound (Janjić, 2002); whereas, it is explicitly defined with the bulk Richardson number in the YSU scheme (Hong et al., 2006):

$$h = R_{ic}\frac{\theta_{vg}u^2(h)}{g[\theta_v(h)-\theta_s]}\ , \tag{5}$$

where R_{ic} is the critical Richardson number; θ_{vg} and $\theta_v(h)$ are the virtual potential temperature at the surface and PBL top, respectively; θ_s is the appropriate potential temperature near the surface, which relates to surface heat fluxes; $u^2(h)$ is the wind speed at the PBL top; and g is the acceleration of gravity.

Although the utility of local schemes can be improved by invoking higher orders of closure in some circumstances (e.g., Mellor and Yamada, 1982; Nakanishi and Niino, 2004; Coniglio et al., 2013), the essential differences in the vertical mixing between different PBL schemes still have a substantial influence on weather processes (Hu et al., 2010; Xie et al., 2012; Cohen et al., 2015), especially for hurricane prediction (Kepert, 2012).

The role of surface-layer schemes is to provide surface exchange coefficients (C_e) to calculate surface fluxes for enthalpy and momentum, and these fluxes are provided as lower boundary conditions for PBL schemes. Under a neutral condition, the surface exchange coefficient can be simplified as

$$C_e = \frac{k^2}{\left[\ln\left(\frac{z_1}{z_0}\right)\right]^2}\ , \tag{6}$$

where k is Von Kármán constant, z_1 denotes the height of the lowest model level and z_0 is the surface roughness, which can be further defined using the Charnock (1955) formula in the case of the ocean surface:

$$z_0 = \frac{\alpha u_*^2}{g}\ , \tag{7}$$

where α is a constant, and u_* is the friction velocity. Considering Eqs. (6) and (7), the surface exchange coefficient (C_e) increases with wind speed (Zhu and Furst, 2013).

In the WRF model, each PBL parameterization is tied to a particular surface-layer scheme. For instance, the MM5 surface-layer similarity (Zhang and Anthes, 1982) is applied along with the YSU PBL, and the Eta surface-layer similarity (Janjić, 1990) is used with the MYJ PBL.

4. Simulation results

4.1. *Track and intensity*

Figure 2a compares the simulated tracks with the NHC best-track data. The simulations with both PBL schemes reproduce tracks that are similar to the best track, while the simulation with the MYJ scheme (simply referred to as MYJ hereafter) performs better than the simulation with the YSU scheme (simply referred to as YSU hereafter) in most cases. Over the ocean in the first 30-h simulation, the simulated track errors are similar in MYJ and YSU (and less than 60 km; Fig. 2b) but become significant after the 30-h simulation. In particular, YSU produces errors that lead to a simulated landfall location about 100 km to the east of the best-track landfall site and a simulated landfall time (around 1400 UTC 29 August 2005) that lags about three hours behind the best-track landfall time (about 1110 UTC 29 August 2005). After landfall, the error enlarges and reaches 100 km. Meanwhile, MYJ reproduces a landfall time and location that are most similar to the best track (about 1110 UTC 29 August 2005), with a track error of only about 30 km when the simulated hurricane makes landfall.

The time series of minimum sea level pressure and maximum surface wind speed (Figs. 2c and d) also indicate that MYJ better predicts the intensity and intensity changes during the simulation period. Specifically, MYJ predicts Katrina (2005)'s RI, especially the minimum sea level pressure drop from 1800 UTC 27 to 1800 UTC 28 August, quite well. The weakening before Katrina (2005)'s landfall (0000 UTC to 1100 UTC 29 August) and the continuous weakening after landfall are also well captured. YSU does predict the RI and also captures the deepening trend, but it produces a shorter period of RI and overall weaker intensity during the simulation period. After landfall, the intensity changes show no obvious differences between the two simulations.

4.2. *Convective structure*

The structure and intensity of precipitation are key factors that characterize hurricane damage, especially for landfalling

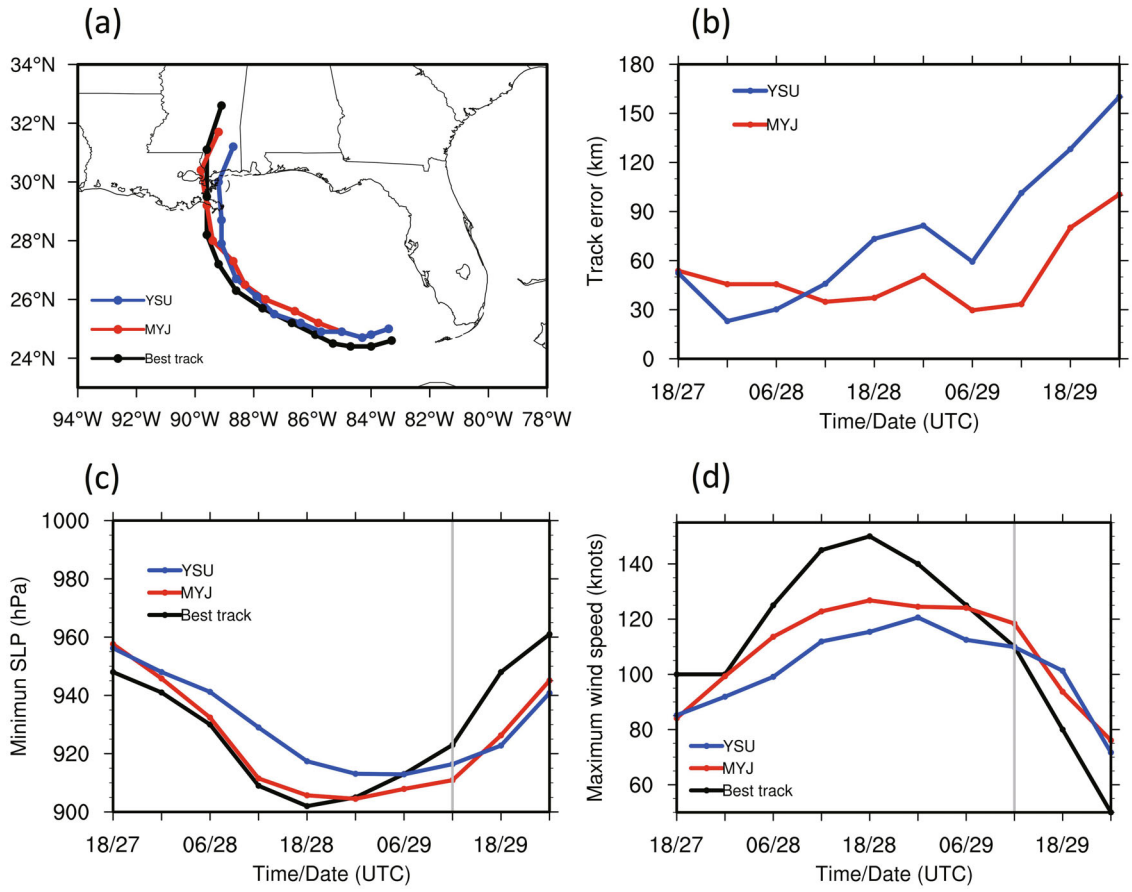

Fig. 2. (a) Comparison of the simulated tracks with the NHC best track with 6-h intervals (the initial time for the black dot is 1800 UTC 27 August). (b) Time series of track errors (units: km) in numerical simulations against the best-track data. (c, d) Time series of (c) minimum sea level pressure (units: hPa) and (d) maximum surface wind (units:kt; 1 kt = 0.5144 m s^{-1}) from the numerical simulations, compared with the NHC best-track data. The time period of the simulations is from 1800 UTC 27 to 0000 UTC 30 August 2005. The vertical gray line in (c) and (d) indicates the landfall time.

hurricanes. Figure 3 compares the simulated radar reflectivity of Katrina (2005) from MYJ and YSU with the convective structure as revealed by composite radar reflectivity from the airborne Doppler radar operated by the NOAA Hurricane Research Division (HRD) near 2000 UTC 27 and a ground-based NEXRAD radar site at New Orleans, LA, at 1352 UTC 29 August 2005. Both simulations produce intense inner and outer rainbands. Specifically, compared with YSU, MYJ produces more organized rainbands. The detailed outer rainband structures from MYJ also more closely resemble the convective structures revealed by radar reflectivity. For instance, at 2000 UTC 27 (Figs. 3a, c and e), MYJ produces a better convective structure near the inner core, which agrees better with the observed inner-core structure, especially in the southeast quadrant of the storm center. YSU, however, produces a weaker storm with more loose structures at this time. At 1400 UTC 29 (Figs. 3b, d and f), YSU reproduces stronger convective intensity in a relatively larger area, compared with observations. These overestimations are ably rectified in MYJ, especially from the south and north to the storm center, where the simulations are quite consistent with the observations.

4.3. *Near-surface winds*

Hurricane damage increases exponentially with low-level wind speed (Elsberry, 2005). Accurate representation of low-level wind structure is an important factor in analyses and forecasts. Figure 4 shows the simulated wind speeds at a height of 10 m, compared with NOAA HRD's surface wind analyses (Powell et al., 2010) (http://www.aoml.noaa.gov/hrd/Storm_pages). At 1200 UTC 28 August, the HRD wind analysis shows a relatively symmetric wind structure around Katrina (2005), with a maximum wind speed in the northeast quadrant of about 130 kt, which is reproduced by MYJ. Although YSU captures the strong wind in the northeast quadrant, the overall wind speed around the vortex is still relatively weaker than the HRD wind analysis and that from MYJ. At 1500 UTC 29 August, shortly after Katrina (2005)'s landfall, the HRD wind analysis illustrates an asymmetric wind structure of Katrina, with a maximum wind speed of 100 kt to the east, which is predicted by both YSU and MYJ. At the same time, compared with the HRD wind analysis, YSU produces wind speeds that are too strong in all quadrants, while MYJ produces wind speeds that are stronger only

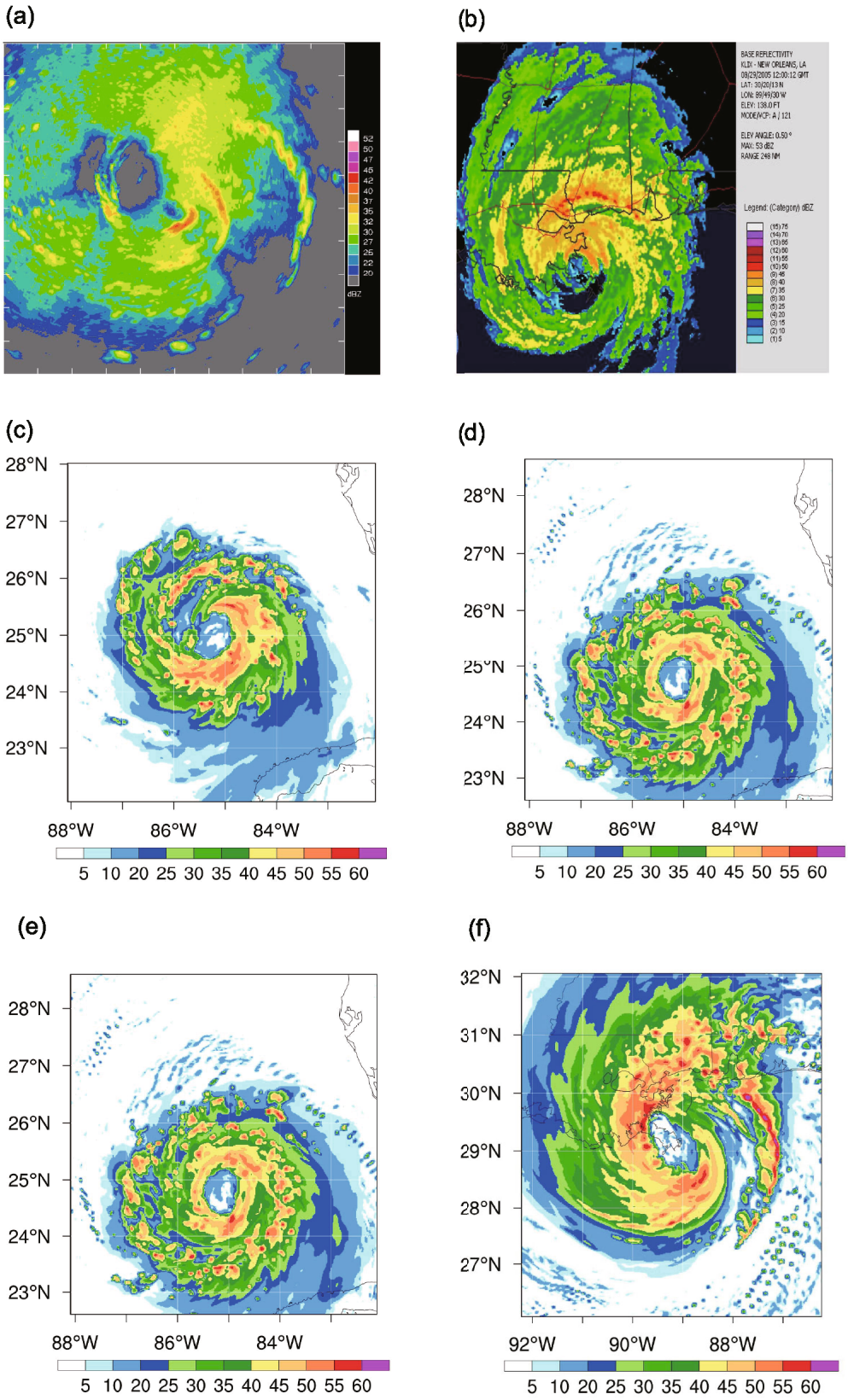

Fig. 3. Composite radar reflectivity from (a) airborne Doppler radar (operated by NOAA/HRD) at 2000 UTC 27 and (b) the ground-based NEXRAD site at New Orleans, LA, at 1352 UTC 29 August 2005. (c, d) and (e, f) illustrate simulated composite radar reflectivity (units: dBZ) at (c, e) 2000 UTC 27 and (d, f) 1400 UTC 29 August 2005 from MYJ and YSU, respectively.

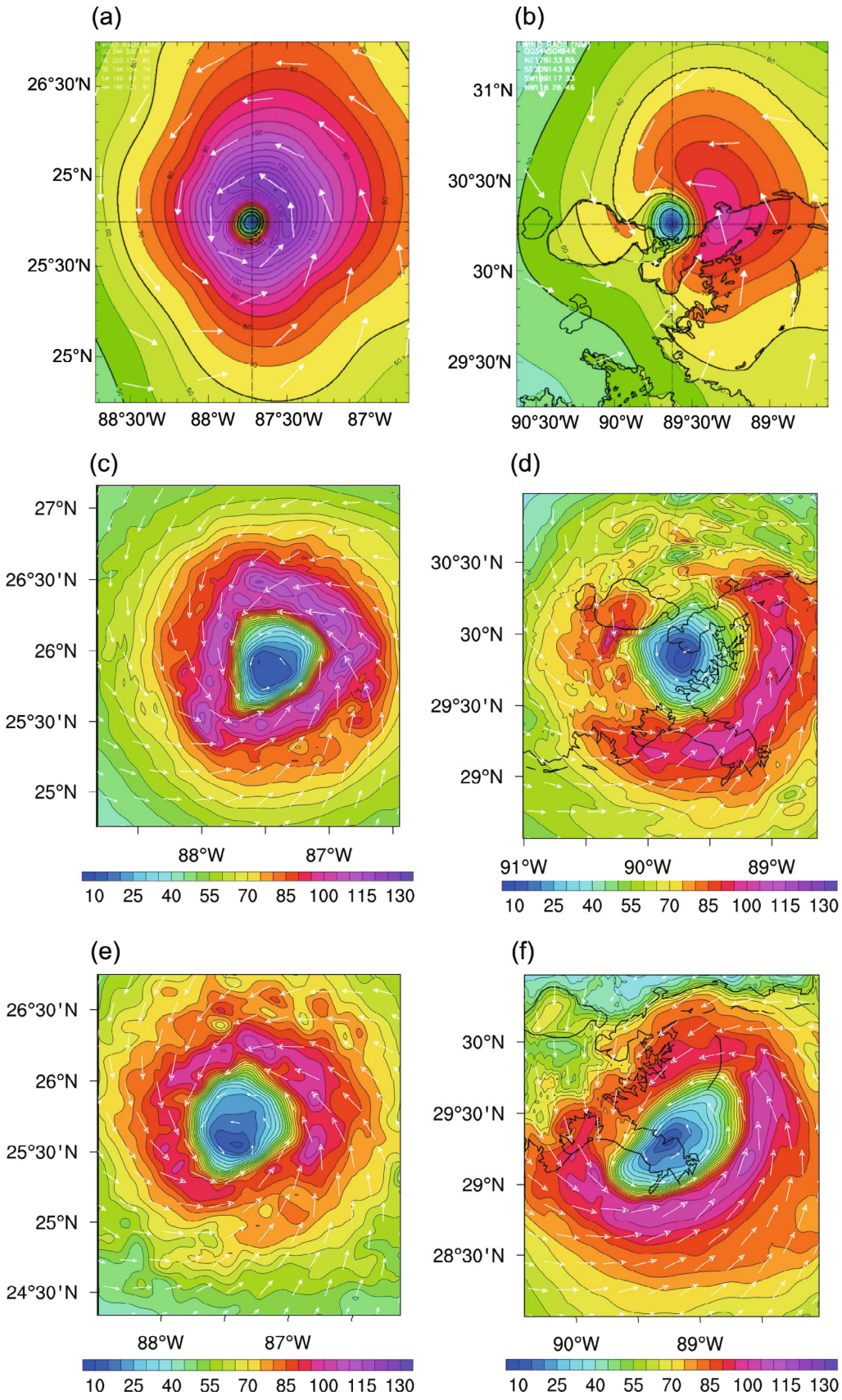

Fig. 4. Near-surface (10 m) wind speeds (shaded contours; units: kt) and wind direction (vectors) at (a, c, e) 1200 UTC 28 and (b, d, f) 1500 UTC 29 August 2005: (a, b) HRD surface wind analysis; (c, d) simulations from MYJ; (e, f) simulations from YSU.

in the south quadrant. Although the inaccurate simulation of wind distribution can be partly attributed to the track errors of the simulations, MYJ outperforms YSU in terms of near-surface wind forecasts overall.

5. Effect of the PBL on RI and evolution

From the simulation results above, it is clear that the use of different PBL schemes has significant effects on the simulation of Katrina (2005)'s track, intensity, and structure. Specifically, significant differences in the intensity between the two simulations appear from 0000 UTC 28 August to 1200 UTC 29 August 2005, with a difference of over 10 hPa in simulated minimum sea level pressure between the two simulations. The simulated hurricane in MYJ intensifies more rapidly than that in YSU and its intensity is also closer to the best-track data, while the simulation with YSU produces a weaker intensity for Katrina (2005) during this RI period. This is similar to results from previous studies (e.g., Li and Pu, 2008; Kepert, 2012), in which higher-order closure schemes, such as the MYJ scheme, lead to better simulations of the hurricane RI process.

To understand the effects of PBL processes on RI, SSTs and surface conditions are examined. Figure 1a shows the SST during Katrina (2005)'s RI before landfall. It is clear that Katrina (2005) passes over a warm SST before its landfall. The SST is relatively higher over the regions where Katrina (2005) moves from and when the RI occurs (Figs. 2c and d), indicating that the pre-existing warm ocean anomaly is crucial to the hurricane's RI process due to the significant increase of air-sea enthalpy fluxes, as revealed by Lin et al. (2009). Moreover, the intensification rate slows down substantially after 1800 UTC 28 August in both simulations (Figs. 2c and d), showing the considerable impact of the land surface on hurricane decay. A similar situation has been revealed by previous studies (Miller, 1964; Rosenthal, 1971; Kimball, 2006), in which the low surface heat and moisture fluxes over land are conducive to hurricane decay during its evolution from ocean to land.

Fundamentally, the PBL scheme transports surface enthalpy (sensible heat and latent heat) and momentum (i.e., friction velocity) fluxes to the boundary layer and free atmosphere, thus providing atmospheric tendencies of temperature, moisture (including clouds), and horizontal momentum in the entire atmospheric column. As mentioned above, the YSU and MYJ PBL schemes, as well as the associated surface-layer scheme, differ in their methodology for calculating the surface fluxes and the vertical mixing in the PBL. Therefore, in order to understand the RI process and also investigate the effects of the PBL schemes on predicting RI, it is necessary to diagnose details regarding the surface enthalpy and momentum fluxes as well as the vertical mixing during the simulation period.

5.1. *Surface enthalpy and momentum fluxes*

Figures 5a and b show the time series of averaged/maximum surface sensible and latent heat fluxes over the vortex core and eyewall regions during the simulation period. The results show that the main discrepancy between the two schemes indeed happens during the RI period. Figure 5a indicates that, although there are only marginal differences in averaged sensible heating between the two simulations over the vortex core region, discrepancies in the maximum values of the surface sensible heat are visible. The simulated surface latent heat fluxes, however, have obvious differences between MYJ and YSU, as shown in Fig. 5b. Specifically, the averaged latent heat flux with MYJ is larger than that with YSU over the vortex core region, especially before Katrina (2005)'s landfall during the RI period. Meanwhile, the maximum value of latent heat in MYJ is also much larger than that in YSU. This is clearly revealed from the horizontal distribution of the moisture fluxes in Fig. 6, which also shows that the surface moisture flux is larger in MYJ than in YSU during the RI period (Figs. 6b and f, and 6c and g, respectively).

Compared with YSU, the larger surface sensible latent heat and moisture fluxes simulated by MYJ during the RI period indicate that the MYJ PBL scheme is more efficient in representing the air–sea interaction as Katrina (2005) passes over the warmer SSTs during the RI period. Meanwhile, the larger surface sensible latent heat and moisture fluxes in MYJ should lead to a high potential for enthalpy transport from the surface to the PBL and free atmosphere, which in turn contributes to the stronger convection (Fig. 3) and stronger hurricane intensity (Figs. 2c and d and Fig. 4) during the RI period. This will be discussed further in the next subsection.

After hurricane landfall, the mean surface sensible heat fluxes become negative (Fig. 5a). The mean surface latent heat fluxes are also close to zero (Fig. 5b). Both of these result in the hurricane's rapid decay due to the great loss of enthalpy energy. Specifically, the surface enthalpy fluxes simulated by the two schemes decrease rapidly and become very similar after hurricane landfall, implying that the MYJ scheme is more sensitive to changes in ocean or land conditions than the YSU scheme, because of its ability to quickly adjust.

Friction velocity is also an important variable in representing the turbulent speeds of the boundary layer and is related to ground stress or vertical momentum flux. The larger the friction velocity, the stronger the mechanical turbulence will be. Moss and Rosenthal (1975) suggested that friction velocity is a key fundamental variable for hurricane development. Figure 5c shows that, on average, the friction velocity simulated with MYJ and YSU is almost the same over the vortex region. Results show that the maximum friction velocity simulated by MYJ is larger than that by YSU during the RI period, resulting in stronger vertical momentum transport in MYJ than in YSU during this period. Accordingly, the maximum wind generated by Katrina (2005) when simulated with MYJ is stronger than that with YSU during the RI period between 0000 UTC 28 August and 1200 UTC 29 August 2005 (see Figs. 2c and d).

Overall, the above results show that the surface enthalpy and momentum fluxes during Katrina (2005)'s RI period produced by MYJ are larger than those by YSU. As a result,

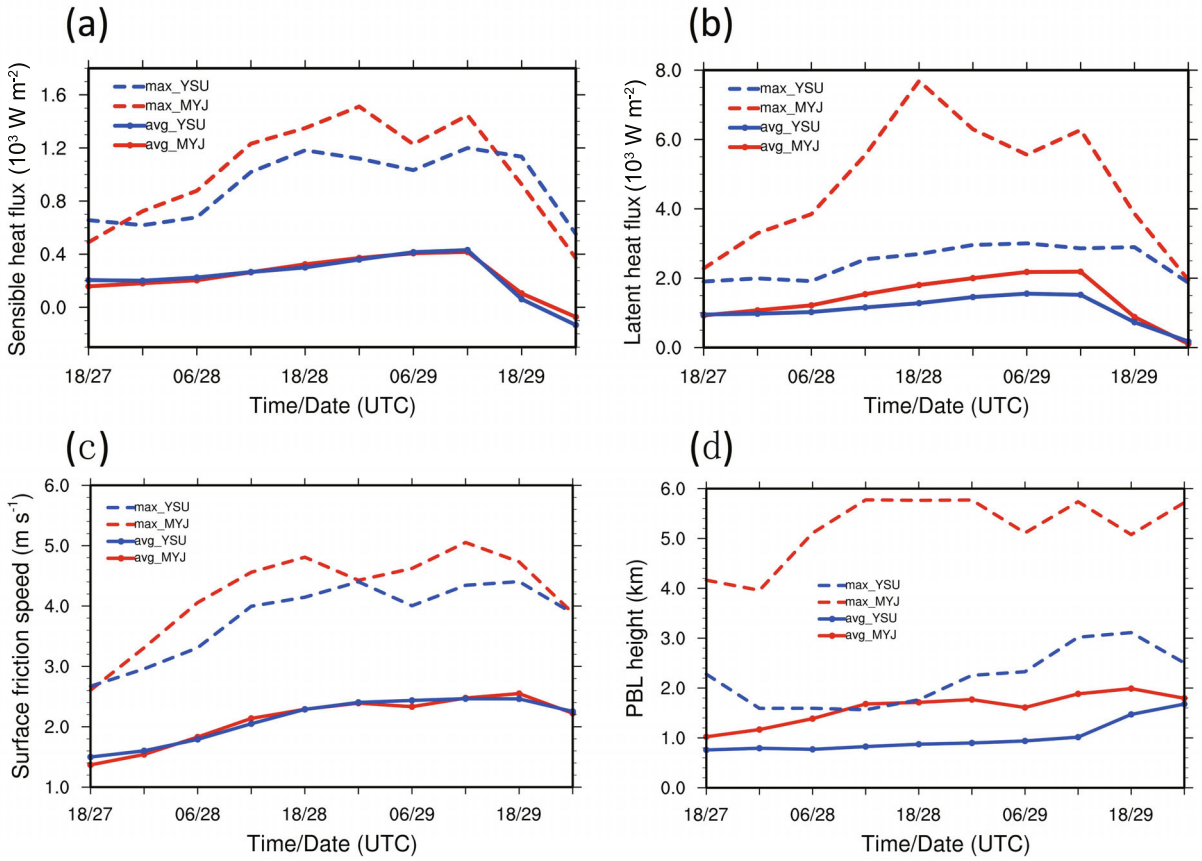

Fig. 5. Time series of (a) surface sensible heat flux (units: 10^3 W m^{-2}), (b) latent heat flux (units: 10^3 W m^{-2}), (c) surface friction velocity speed (units: m s^{-1}), and (d) boundary layer height (units: km), averaged over an area within a radius of 150 km from the storm center.

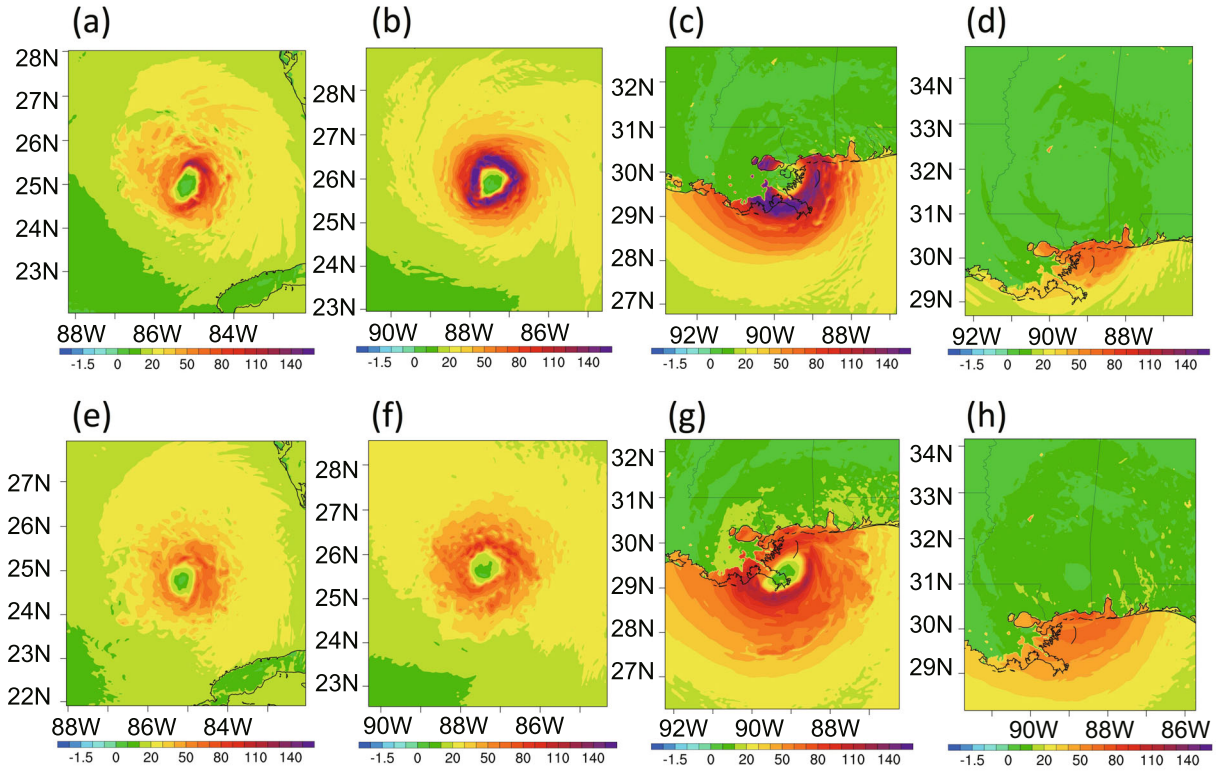

Fig. 6. Surface moisture flux (units: 10^{-5} kg m^{-2} s^{-1}) at (a, e) 2000 UTC 27, (b, f) 1200 UTC 28, (c, g) 1500 UTC 29, and (d, h) 0000 UTC 30 August 2005, from (a–d) MYJ and (e–h) YSU.

MYJ produces an improved hurricane RI process, compared to the weaker hurricane intensity in YSU. Similar results are demonstrated in Braun and Tao (2000).

5.2. *Vertical mixing in the PBL and its effects*

As discussed in the previous section, the larger surface fluxes in MYJ should lead to a high potential for enthalpy transport from the surface to the PBL and free atmosphere. In fact, as mentioned in section 3, the MYJ scheme and the YSU scheme differ in their treatments of vertical diffusion, and this could create discrepancies in the vertical structure of the hurricane in the PBL. Therefore, the interactions between surface fluxes and vertical mixing in the PBL, as well as the evolution of hurricane vortices and their boundary layer structures, are examined in this subsection.

Figure 5d shows the time series of the maximum value and averaged PBLH over the simulated hurricane core and eyewall regions during the whole simulation period. Apparently, MYJ produces a higher PBLH than YSU. The maximum PBLH produced by MYJ can be extended higher than 5 km vertically, while the maximum PBLH generated by YSU remains below 3 km in height. The higher PBLH in MYJ implies stronger vertical mixing in the simulation with the MYJ PBL scheme (shown in Fig. 7), and this is consistent with the results of Zhang et al. (2015), who found that strong vertical mixing corresponds to a high PBLH. Specifically, the simulated mean and maximum PBLH in MYJ are much higher than in YSU during the RI period, indicating that there is much stronger vertical mixing in MYJ during this period. This stronger vertical mixing should enable the efficient transport of a large amount of surface momentum and enthalpy flux to the hurricane boundary layer, thereby enhancing hurricane development.

Figure 7 examines the vertical mixing in the two schemes during the hurricane RI period by comparing the vertical exchange coefficients in YSU and MYJ. It clearly shows that the vertical mixing in MYJ is stronger than that in YSU, as the vertical exchange coefficients in MYJ are stronger and extend to over 800 hPa, approximately, at both 1200 UTC 28 and 0000 UTC 29 August 2005, corresponding to the higher PBLH (Fig. 5d) at those times. At the same time, the vertical mixing in YSU remains mostly in the vertical levels below the 850 hPa pressure level.

Figures 8 and 9 illustrate the azimuthally averaged temperature anomalies and tangential and radial winds from the simulated hurricane center to a radius of 300 km, clearly revealing that the simulated hurricane in MYJ is stronger and has stronger tangential winds, inflow/outflow, and warm-core center than that in YSU. It seems that the stronger vertical mixing in MYJ yields stronger hurricane intensity and

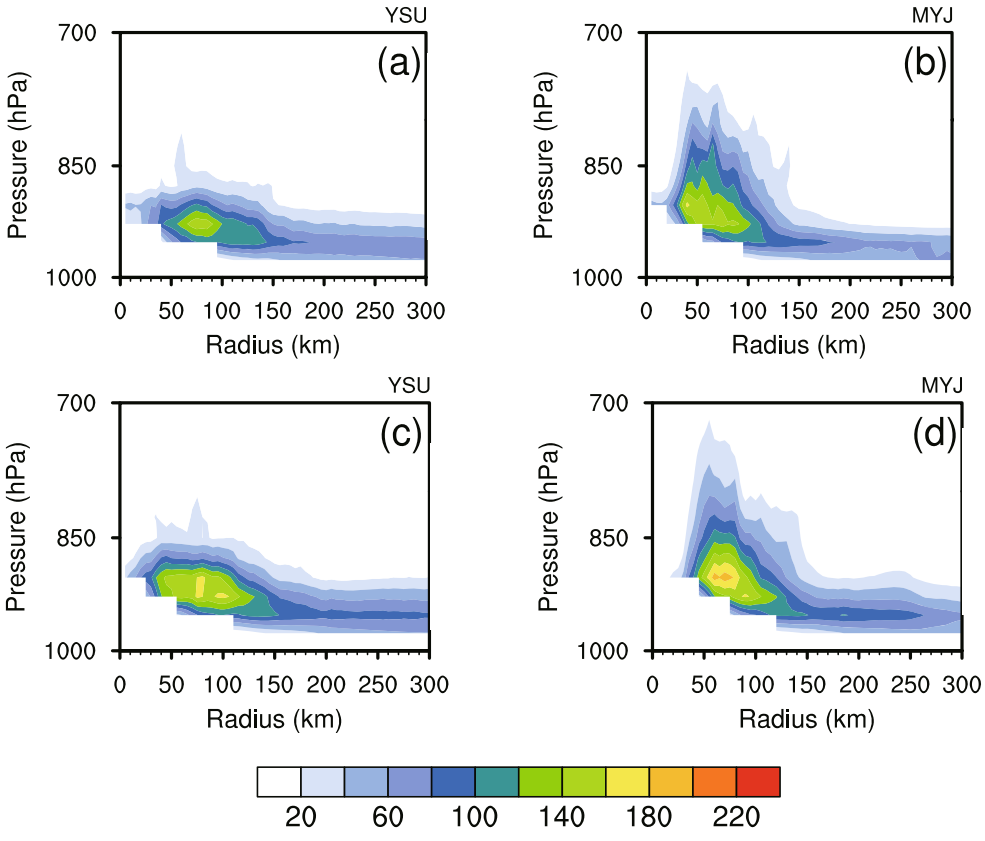

Fig. 7. Azimuthally averaged vertical exchange coefficients with a radius of 300 km from the storm center in the (a, c) YSU and (b, d) MYJ schemes, at (a, b) 1200 UTC 28 August 2005 and (c, d) 0000 UTC 29 August 2005.

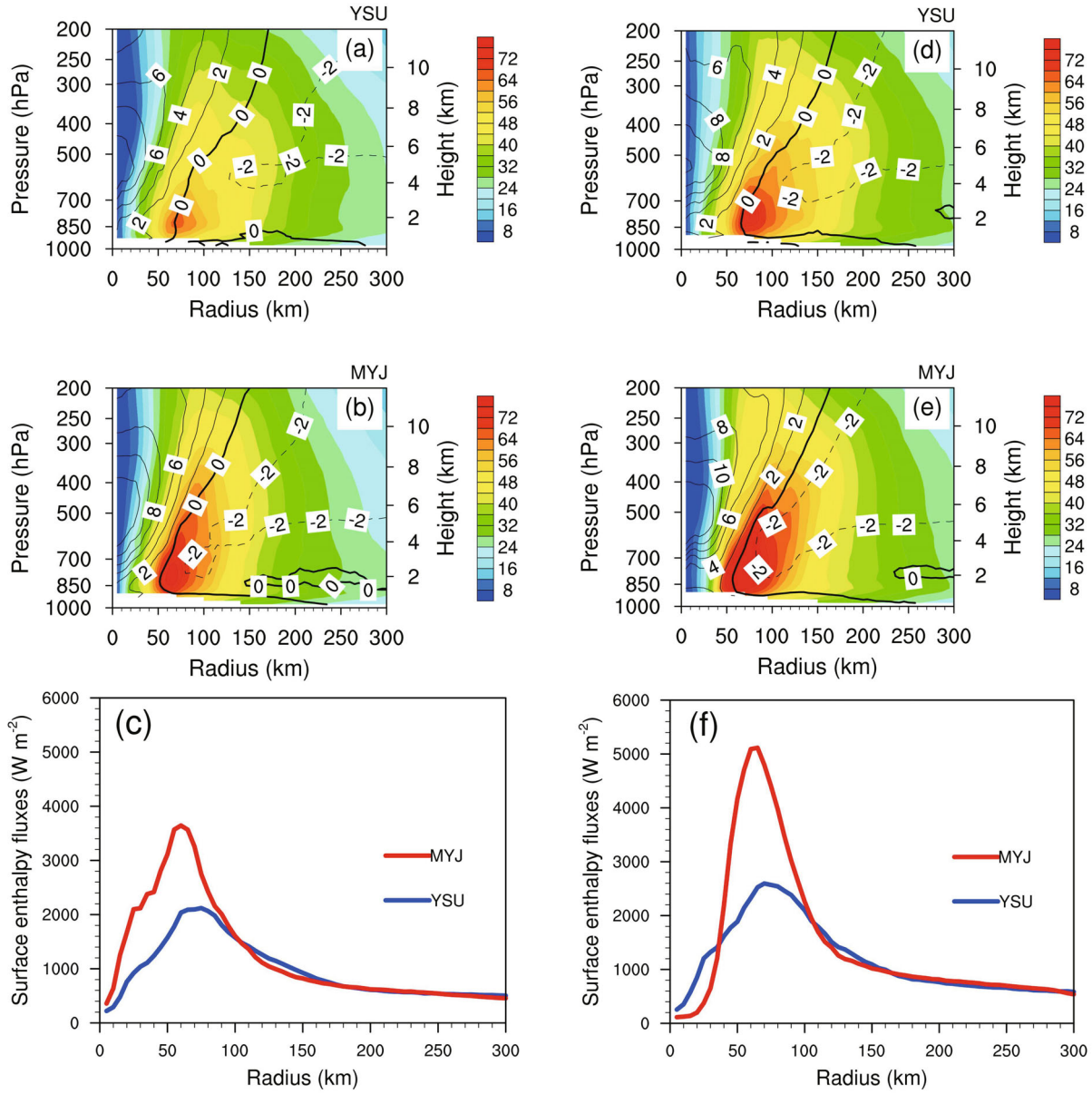

Fig. 8. Azimuthally averaged temperature anomalies (contours) and tangential wind speed (color-shaded) from 1000 hPa to 200 hPa, in the (a, b) YSU and (d, e) MYJ schemes, at (a, d) 1200 UTC 28 August 2005 and (b, e) 0000 UTC 29 August 2005. The surface enthalpy fluxes (units: W m^{-2}) at (c) 1200 UTC 28 August 2005 and (f) 0000 UTC 29 August 2005 in the two schemes are also provided.

higher wind speeds, indicating more efficient air–sea interactions as Hurricane Katrina (2005) passes the warm SST regions. According to Eqs. (6) and (7), the surface fluxes depend on the wind speed, and the surface exchange coefficient also increases with the wind speed. At the same time, the larger amount of surface fluxes (Figs. 5 and 6) from MYJ is also conducive to hurricane development. Thus, the positive feedback between vertical mixing and surface fluxes in MYJ eventually results in a stronger hurricane vortex than that in YSU. In other words, the stronger surface enthalpy and momentum fluxes, as well as the stronger vertical mixing produced by the MYJ scheme during the hurricane RI period, are the main reasons for a stronger warm core and tangential winds (Fig. 8). This is consistent with the results of Miyamoto and Takemi (2013), who found that the efficient transport of enthalpy from the underlying ocean to a hurricane is an essential triggering mechanism of hurricane RI.

5.3. *Divergence and eyewall contraction*

To further examine the corresponding changes in the hurricane vortices in the two PBL schemes, Fig. 10a illustrates the vertical profiles of averaged convergence/divergence over the simulated hurricane core and eyewall regions from 0000 UTC 28 to 1200 UTC 29 August 2005. It shows that MYJ predicts a hurricane vortex with stronger convergence at 3–6 km and divergence at 10–15 km. Specifically, the low-

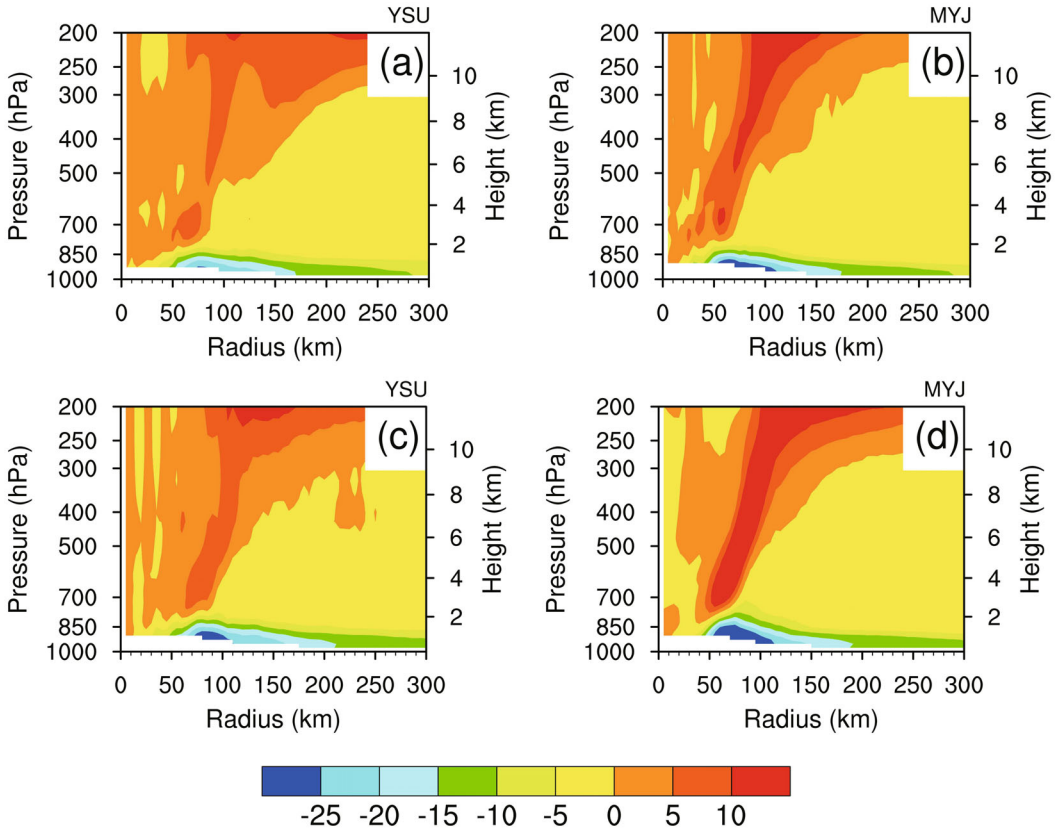

Fig. 9. As in Fig. 7 but for the radial wind speed from 1000 hPa to 200 hPa.

level vortex convergence in MYJ extends to about 7 km, while at the same time the magnitude of the low-level convergence in YSU is much weaker, extending to only about 6 km. The stronger convergence and divergence in MYJ should correspond to more intense inflow and outflow, resulting in a stronger hurricane during this period, and this is also consistent with the more reasonable surface wind and pressure, as shown in Figs. 2c and d.

The radius of maximum wind usually contracts as a hurricane intensifies (Willoughby, 1990). Based on 900 radial profiles from aircraft observations of 19 Atlantic TCs, Willoughby (1990) found that the contraction of the storm eyewall could be the primary symptom of hurricane intensification. Eyewall contraction, accompanied by higher tangential winds, could cause more moisture and energy to be extracted from the ocean surface and transported into the hurricane eyewall. In order to compare the eyewall contraction during the RI period in numerical simulations of Katrina (2005) , Fig. 10b shows the wind speed at 850 hPa along the longitude through the hurricane centers averaged over 0000 UTC 28 to 1200 UTC 29 August 2005 (the RI period). It indicates that Katrina (2005) experiences more intense eyewall contraction in MYJ than in YSU during the RI period, confirming that RI is stronger in MYJ.

In addition, using an idealized simulation, Stern et al. (2015) proved that heating and friction both contribute substantially to boundary layer inflow; thus they also both contribute to the contraction of the radius of maximum wind (eyewall contraction). Therefore, the different characteristics of divergence and eyewall contractions related to the hurricane RI period in the two simulations in this study can be attributed to the differences in surface enthalpy (sensible and latent heating) and momentum (frictional velocity) fluxes and vertical mixing (i.e., PBLH) generated by the two simulations with different PBL schemes.

6. Summary and concluding remarks

In this study, numerical simulations of an RI period before Katrina Katrina (2005)'s second landfall in Louisiana, USA, are performed. The sensitivity of numerical simulations to two widely used PBL schemes, MYJ and YSU, is examined. The effects of surface momentum and enthalpy fluxes, as well as vertical mixing in the PBL, on hurricane RI processes before landfall are discussed. We find that the different surface momentum, enthalpy, and vertical mixing in the PBL resulting from the use of the YSU and MYJ schemes can have fundamental effects on hurricane track and intensity changes. The major findings can be summarized as follows:

(1) Compared with the NHC best-track data, the simulation with the MYJ scheme reproduces better track forecasts with a more accurate landfall time and location, as well as a better intensity forecast in terms of the temporal variation of minimum sea level pressure and maximum wind, than the

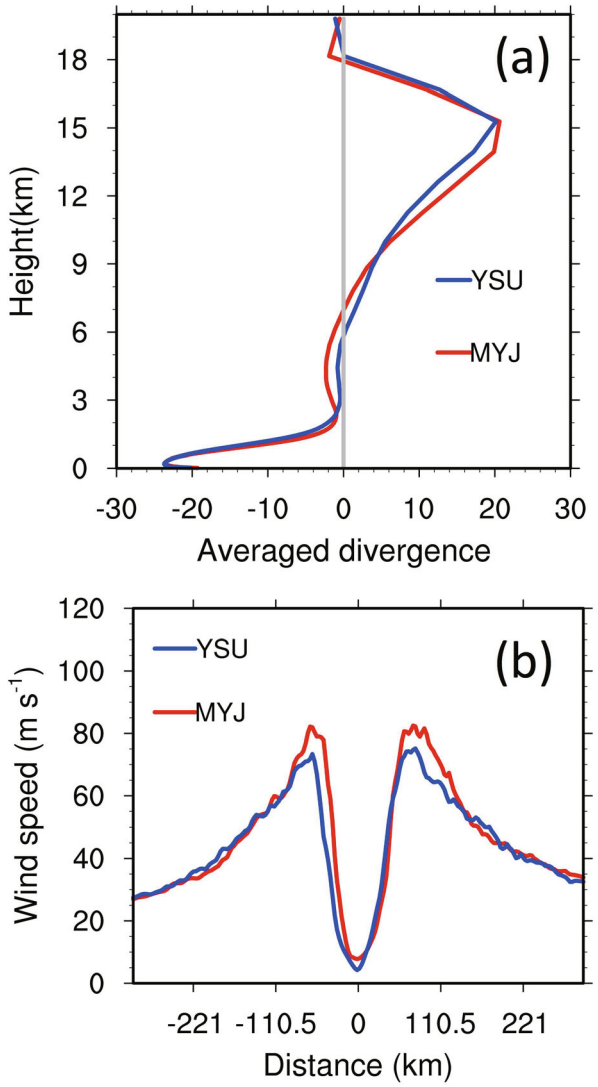

Fig. 10. (a) Composite mean divergence profiles over an area of 150 km radius around the simulated hurricane center at different times. The horizontal axis represents the magnitude of the divergence (units: 10^{-4} s^{-1}). (b) Composite mean wind speed at 850 hPa along the longitude through the hurricane centers. In both panels the composite represents the period from 0000 UTC 28 to 1200 UTC 29 August 2005 (the RI period).

simulation with the YSU scheme. In addition, compared with airborne Doppler radar observations and HRD wind analyses, the simulation with the MYJ scheme also reproduces more reasonable precipitation and near-surface wind structure for Katrina (2005) than the simulation with YSU.

(2) Large discrepancies in intensity forecasts (e.g., about 10 hPa differences in minimum sea level pressure) are found in the two simulations during the RI period.

(3) Further diagnoses indicate that, compared to the simulation with the YSU PBL scheme, the simulation with the MYJ scheme generates stronger surface enthalpy and momentum fluxes, reflecting more efficient air–sea interaction when Hurricane Katrina (2005) passes over regions with warm SSTs. Meanwhile, the MYJ scheme also leads to stronger vertical mixing, which causes a higher PBLH and a stronger hurricane warm core and radial/tangential winds during the hurricane RI period, resulting in a stronger vortex and a more intense (and comparable to observation) simulation of Hurricane Katrina (2005).

(4) The divergence and eyewall contraction during the RI period further indicate that the simulation with the MYJ scheme produces more intense convergence in the lower to middle atmosphere and more intense divergence in the upper level, as well as more intense eyewall contraction. These characteristics, however, are not obvious in the YSU scheme.

Although the two PBL schemes lead to different predictions of Hurricane Katrina (2005) before its landfall, it should be noted that the results of this study should not be used as a commentary on which scheme is better, since this is only a case study. However, previous studies (Li and Pu, 2008; Nolan et al., 2009) have also shown that simulations with the MYJ PBL scheme are better at portraying hurricane RI than those with the YSU PBL scheme. Moreover, based on an idealized diagnostic TC model, Kepert (2012) recommended that higher-order closure schemes, such as the MYJ scheme, are more suitable for hurricane simulation.

Overall, outcomes from this study demonstrate the importance of the PBL scheme in numerical predictions of hurricane RI. Specifically, this study suggests that better representation of surface fluxes and vertical mixing in the PBL is essential for accurate prediction of hurricane intensity changes. In addition, a recent study by Rotunno and Bryan (2012) highlighted the importance of horizontal diffusion for maximum simulated hurricane intensity. Future work should emphasize more case studies with an atmosphere–ocean coupled model, as well as horizontal diffusion parameterization, to obtain deeper understanding of hurricane RI processes before landfall.

Acknowledgements. This study was supported by the US National Science Foundation (Grant No. AGS-1243027). Computer support from the Center for High-Performance Computing at the University of Utah is appreciated. In addition, high-performance computing support from Yellowstone (ark:/85065/d7wd3xhc), provided by NCAR's Computational and Information Systems Laboratory and sponsored by the National Science Foundation, is also acknowledged. Comments from Prof. Ming XUE and two anonymous reviewers were very helpful for improving the manuscript.

REFERENCES

Black, P. G., and Coauthors, 2007: Air-sea exchange in hurricanes: Synthesis of observations from the Coupled Boundary Layer Air-Sea Transfer experiment. *Bull. Amer. Meteor. Soc.*, **88**, 357–374.

Bosart, L. F., W. E. Bracken, J. Molinari, C. S. Velden, and P. G. Black, 2000: Environmental influences on the rapid intensification of Hurricane Opal (1995) over the Gulf of Mexico. *Mon. Wea. Rev.*, **128**, 322–352.

Braun, S. A., and W. K. Tao, 2000: Sensitivity of high-resolution simulations of Hurricane Bob (1991) to planetary boundary

layer parameterizations. *Mon. Wea. Rev.*, **128**, 3941–3961.

Cecil, D. J., and E. J. Zipser, 1999: Relationships between tropical cyclone intensity and satellite-based indicators of inner core convection: 85-GHz ice-scattering signature and lightning. *Mon. Wea. Rev.*, **127**(1), 103–123.

Charnock, H., 1955: Wind stress on a water surface. *Quart. J. Roy. Meteor. Soc.*, **81**(350), 639–640.

Chen, F., and J. Dudhia, 2001: Coupling an advanced land surface-hydrology model with the Penn State-NCAR MM5 modeling system. Part I: Model implementation and sensitivity. *Mon. Wea. Rev.*, **129**, 569–585.

Cohen, A. E., S. M. Cavallo, M. C. Coniglio, and H. E. Brooks, 2015: A review of planetary boundary layer parameterization schemes and their sensitivity in simulating southeastern U.S. cold season severe weather environments. *Wea. Forecasting*, **30**(3), 591–612.

Coniglio, M. C., J. Correia, P. T. Marsh, and F. Y. Kong, 2013: Verification of convection-allowing WRF model forecasts of the planetary boundary layer using sounding observations. *Wea. Forecasting*, **28**, 842–862.

Davis, C., and L. F. Bosart, 2002: Numerical simulations of the genesis of Hurricane Diana (1984). Part II: Sensitivity of track and intensity prediction. *Mon. Wea. Rev.*, **130**, 1100–1124.

DeMaria, M., R. T. DeMaria, J. A. Knaff, and D. Molenar, 2012: Tropical cyclone lightning and rapid intensity change. *Mon. Wea. Rev.*, **140**, 1828–1842.

Dudhia, J., 1989: Numerical study of convection observed during the Winter Monsoon Experiment using a mesoscale two-dimensional model. *J. Atmos. Sci.*, **46**, 3077–3107.

Elsberry, R. L., 2005: Achievement of USWRP hurricane landfall research goal. *Bull. Amer. Meteor. Soc.*, **86**, 643–645.

Elsberry, R. L., L. S. Chen, J. Davidson, R. Rogers, Y. Q. Wang, and L. G. Wu, 2013: Advances in understanding and forecasting rapidly changing phenomena in tropical cyclones. *Tropical Cyclone Research Review*, **2**, 13–24.

Fierro, A. O., X. M. Shao, T. Hamlin, J. M. Reisner, and J. Harlin, 2011: Evolution of eyewall convective events as indicated by intracloud and cloud-to-ground lightning activity during the rapid intensification of Hurricanes Rita and Katrina. *Mon. Wea. Rev.*, **139**, 1492–1504.

Frank, W. M., 1977: The structure and energetics of the tropical cyclone II: Dynamics and energetics. *Mon. Wea. Rev.*, **105**, 1136–1150.

Frank, W. M., and E. A. Ritchie, 1999: Effects of environmental flow upon tropical cyclone structure. *Mon. Wea. Rev.*, **127**, 2044–2061.

Gall, R., J. Franklin, F. Marks, E. N. Rappaport, and F. Toepfer, 2013: The hurricane forecast improvement project. *Bull. Amer. Meteor. Soc.*, **94**, 329–334.

Gray, W. M., 1968: Global view of the origin of tropical disturbances and storms. *Mon. Wea. Rev.*, **96**, 669–700.

Guimond, S. R., G. M. Heymsfield, and F. J. Turk, 2010: Multiscale observations of Hurricane Dennis (2005): The effects of hot towers on rapid intensification. *J. Atmos. Sci.*, **67**, 633–654.

Hendricks, E. A., M. T. Montgomery, and C. A. Davis, 2004: The role of "vortical" hot towers in the formation of Tropical Cyclone Diana (1984). *J. Atmos. Sci.*, **61**, 1209–1232.

Hong, S.-Y., and J.-O. J. Lim, 2006: The WRF single-moment 6-class microphysics scheme (WSM6). *Journal of the Korean Meteorological Society*, **42**, 129–151.

Hong, S.-Y., Y. Noh, and J. Dudhia, 2006: A new vertical diffusion package with an explicit treatment of entrainment processes. *Mon. Wea. Rev.*, **134**, 2318–2341.

Houze, R. A. Jr., and Coauthors, 2006: The hurricane rainband and intensity change experiment: Observations and modeling of hurricanes Katrina, Ophelia, and Rita. *Bull. Amer. Meteor. Soc.*, **87**, 1503–1521.

Hu, X. M., J. W. Nielsen-Gammon, and F. Q. Zhang, 2010: Evaluation of three planetary boundary layer schemes in the WRF model. *Journal of Applied Meteorology and Climatology*, **49**(9), 1831–1844.

Janjić, Z. I., 1990: The step-mountain coordinate: Physical package. *Mon. Wea. Rev.*, **118**, 1429–1443.

Janjić, Z. I., 2002: Nonsingular implementation of the Mellor-Yamada level 2.5 scheme in the NCEP Meso model. NCEP Office Note 437, 61 pp. [Available at NCEP/EMC, 5200 Auth Road, Camp Springs, MD 20746.]

Jiang, H. Y., 2012: The relationship between tropical cyclone intensity change and the strength of inner-core convection. *Mon. Wea. Rev.*, **140**, 1164–1176.

Jiang, H. Y., C. T. Liu, and E. J. Zipser, 2011: A TRMM-based tropical cyclone cloud and precipitation feature database. *Journal of Applied Meteorology and Climatology*, **50**, 1255–1274.

Kain, J. S., and J. M. Fritsch, 1993: Convective parameterization for mesoscale models: The Kain-Fritsch scheme. *The Representation of Cumulus Convection in Numerical Models*, K. A. Emanuel and D. J. Raymond, Eds., American Meteorological Society, 165–170.

Kaplan, J., and M. DeMaria, 2003: Large-scale characteristics of rapidly intensifying tropical cyclones in the North Atlantic basin. *Wea. Forecasting*, **18**, 1093–1108.

Kaplan, J., M. DeMaria, and J. A. Knaff, 2010: A revised tropical cyclone rapid intensification index for the Atlantic and eastern North Pacific basins. *Wea. Forecasting*, **25**, 220–241.

Karyampudi, V. M., G. S. Lai, and J. Manobianco, 1998: Impact of initial conditions, rainfall assimilation, and cumulus parameterization on simulations of Hurricane Florence (1988). *Mon. Wea. Rev.*, **126**, 3077–3101.

Kelley, O. A., J. Stout, and J. B. Halverson, 2004: Tall precipitation cells in tropical cyclone eyewalls are associated with tropical cyclone intensification. *Geophys. Res. Lett.*, **31**, L24112.

Kelley, O. A., J. Stout, and J. B. Halverson, 2005: Hurricane intensification detected by continuously monitoring tall precipitation in the eyewall. *Geophys. Res. Lett.*, **32**, L20819.

Kepert, J. D., 2012: Choosing a boundary layer parameterization for tropical cyclone modeling. *Mon. Wea. Rev.*, **140**(5), 1427–1445.

Kieper, M. E., and H. Y. Jiang, 2012: Predicting tropical cyclone rapid intensification using the 37 GHz ring pattern identified from passive microwave measurements. *Geophys. Res. Lett.*, **39**, L13804.

Kimball, S. K., 2006: A modeling study of hurricane landfall in a dry environment. *Mon. Wea. Rev.*, **134**(7), 1901–1918.

Landsea, C. W., 1993: A climatology of intense (or major) Atlantic hurricanes. *Mon. Wea. Rev.*, **121**, 1703–1713.

Li, X. L., and Z. X. Pu, 2008: Sensitivity of numerical simulation of early rapid intensification of Hurricane Emily (2005) to cloud microphysical and planetary boundary layer parameterizations. *Mon. Wea. Rev.*, **136**, 4819–4838.

Lin, I.-I., C.-H. Chen, I.-F. Pun, W. T. Liu, and C.-C. Wu, 2009: Warm ocean anomaly, air sea fluxes, and the rapid intensification of Tropical Cyclone Nargis (2008). *Geophys. Res. Lett.*,

36, L03817.

Malkus, J. S., 1958: On the structure and maintenance of the mature hurricane eye. *J. Meteor.*, **15**, 337–349.

Marks, F. D., and L. K. Shay, 1998: Landfalling tropical cyclones: Forecast problems and associated research opportunities. *Bull. Amer. Meteor. Soc.*, **79**(2), 305–323.

Mellor, G. L., and T. Yamada, 1982: Development of a turbulence closure model for geophysical fluid problems. *Rev. Geophys.*, **20**, 851–875.

Miller, B. I., 1964: A study of the filling of Hurricane Donna (1960) over land. *Mon. Wea. Rev.*, **92**(9), 389–406.

Miyamoto, Y., and T. Takemi, 2013: A transition mechanism for the spontaneous axisymmetric intensification of tropical cyclones. *J. Atmos. Sci.*, **70**, 112–129.

Mlawer, E. J., S. J. Taubman, P. D. Brown, M. J. Iacono, and S. A. Clough, 1997: Radiative transfer for inhomogeneous atmospheres: RRTM, a validated correlated-k model for the longwave. *J. Geophys. Res.*, **102**, 16 663–16 682.

Montgomery, M. T., M. E. Nicholls, T. A. Cram, and A. B. Saunders, 2006a: A vortical hot tower route to tropical cyclogenesis. *J. Atmos. Sci.*, **63**, 355–386.

Montgomery, M. T., M. M. Bell, S. D. Aberson, and M. L. Black, 2006b: Hurricane Isabel (2003): New insights into the physics of intense storms. Part I: Mean vortex structure and maximum intensity estimates. *Bull. Amer. Meteor. Soc.*, **87**, 1335–1347.

Moss, M. S. and S. L. Rosenthal, 1975: On the estimation of planetary boundary layer variables in mature hurricanes. *Mon. Wea. Rev.*, **103**, 980–988.

Nakanishi, M., and H. Niino, 2004: An improved Mellor-Yamada level-3 model with condensation physics: Its design and verification. *Bound.-Layer Meteor.*, **112**, 1–31.

Noh, Y., W. G. Cheon, S. Y. Hong, and S. Raasch, 2003: Improvement of the K-profile model for the planetary boundary layer based on large eddy simulation data. *Bound.-Layer Meteor.*, **107**, 401–427.

Nolan, D. S., D. P. Stern, and J. A. Zhang, 2009: Evaluation of planetary boundary layer parameterizations in tropical cyclones by comparison of in situ observations and high-resolution simulations of Hurricane Isabel (2003). Part II: Inner-core boundary layer and eyewall structure. *Mon. Wea. Rev.*, **137**, 3675–3698.

Pielke, R. A. Jr., and R. A. Pielke Sr., 1997: *Hurricanes*: *Their Nature and Impacts on Society*. John Wiley and Sons, 298 pp.

Powell, M. D., and Coauthors, 2010: Reconstruction of Hurricane Katrina's wind fields for storm surge and wave hindcasting. *Ocean Engineering*, **37**, 26–36.

Rogers, R., and Coauthors, 2006: The intensity forecasting experiment: A NOAA multiyear field program for improving tropical cyclone intensity forecasts. *Bull. Amer. Meteor. Soc.*, **87**, 1523–1537.

Rogers, R. F., and Coauthors, 2013: NOAA's Hurricane Intensity Forecasting Experiment: A progress report. *Bull. Amer. Meteor. Soc.*, **94**, 859–882.

Rosenthal, S. L., 1971: The response of a tropical cyclone model to variations in boundary layer parameters, initial conditions, lateral boundary conditions, and domain size. *Mon. Wea. Rev.*, **99**(10), 767–777.

Rotunno, R., and G. H. Bryan, 2012: Effects of parameterized diffusion on simulated hurricanes. *J. Atmos. Sci.*, **69**(7), 2284–2299.

Skamarock, W. C., and Coauthors, 2008: A description of the advanced research WRF version 3. Tech. Note NCAR/TN-475+STR, 113 pp. [Available online at http://www2.mmm.ucar.edu/wrf/users/docs/arw_v3.pdf.]

Smith, R. K., and G. L. Thomsen, 2010: Dependence of tropical-cyclone intensification on the boundary-layer representation in a numerical model. *Quart. J. Roy. Meteor. Soc.*, **136**, 1671–1685.

Stern, D. P., J. L. Vigh, D. S. Nolan, and F. Q. Zhang, 2015: Revisiting the relationship between eyewall contraction and intensification. *J. Atmos. Sci.*, **72**, 1283–1306.

Troen, I. B., and L. Mahrt, 1986: A simple model of the atmospheric boundary layer: Sensitivity to surface evaporation. *Bound.-Layer Meteor.*, **37**, 129–148.

Willoughby, H. E., 1988: The dynamics of the tropical cyclone core. *Aust. Meteor. Mag.*, **36**, 183–191.

Willoughby, H. E., 1990: Temporal changes of the primary circulation in tropical cyclones. *J. Atmos. Sci.*, **47**, 242–264.

Xie, B., J. C. H. Fung, A. Chan, and A. Lau, 2012: Evaluation of nonlocal and local planetary boundary layer schemes in the WRF model, *J. Geophys. Res.*, **117**, D12103.

Zhang, D. L., and R. A. Anthes, 1982: A high-resolution model of the planetary boundary layer-sensitivity tests and comparisons with SESAME-79 data. *J. Appl. Meteor.*, **21**, 1594–1609.

Zhang, J. A., D. S. Nolan, R. F. Rogers, and V. Tallapragada, 2015: Evaluating the impact of improvements in the boundary layer parameterization on hurricane intensity and structure forecasts in HWRF. *Mon. Wea. Rev.*, **143**, 3136–3155.

Zhu, P., and J. Furst, 2013: On the Parameterization of Surface Momentum Transport via Drag Coefficient in Low Wind Conditions. *Geophy. Res. Lett.*, **40**, 2824-2828.

Zhu, P., K. Menelaou, and Z. D. Zhu, 2014: Impact of subgrid-scale vertical turbulent mixing on eyewall asymmetric structures and mesovortices of hurricanes. *Quart. J. Roy. Meteor. Soc.*, **140**, 416–438.